Supporting Information

In situ lignin adhesion for high-performance bamboo composites

Taotao Meng[1a], Yu Ding[1a], Yu Liu[1], Lin Xu[1], Yimin Mao[1,2], Julia Gelfond[1,3], Shuke Li[1], Zhihan Li[1], Paul F. Salipante[4], Hoon Kim[5], J.Y. Zhu [5], Xuejun Pan[6,*], Liangbing Hu[1,*]

[1]Department of Materials Science and Engineering, University of Maryland, College Park, MD 20742

[2] NIST Center for Neutron Research, National Institute of Standards and Technology, Gaithersburg, MD 20899

[3]Montgomery Blair High School, Silver Spring, MD 20901

[4]Polymers and Complex Fluids Group, National Institute of Standards and Technology, Gaithersburg, MD 20899

[5]U.S. Department of Agriculture, Forest Service, Forest Products Laboratory, Madison, WI 53726

[6]Department of Biological Systems Engineering, University of Wisconsin-Madison, Madison, WI 53706

[*] Email: binghu@umd.edu; xpan@wisc.edu

[a] These authors contributed equally to this work.

Methods

Materials and chemicals Raw bamboo (*Phyllostachys edulis*) was purchased from Worown, Inc., United States. NaOH (>98%) was purchased from Sigma-Aldrich.

Fabrication process of *in situ* glubam First, natural bamboo strips (40.0 mm by 10.0 mm by 2.0 mm) were immersed in 20 wt% NaOH aqueous solution for 12 hours under vacuum. The bamboo strips were then autoclaved at 160 ℃ for 1 hour, and finally immersed in deionized water several times to remove the residual chemicals, dissolved lignin and hemicellulose. The two pieces of bamboo strips were pressed at different temperatures (120, 140, 160, and 180 ℃) for 20 minutes under a pressure of about 20 MPa to produce *in situ* glubam. *In situ* glubam with varying degrees of lignin removal can be obtained by adjusting the autoclaving time.

Characterization The bamboo samples were characterized using a scanning electron microscope (SEM, Tescan XEIA). Fourier transform infrared spectroscopy (FTIR) was performed on a Thermo Nicolet Nexus 6700 spectrometer to determine the functional groups of bamboo samples. The acid hydrolysis method was used to analyze the compositional content of the bamboo samples, and the acid-insoluble lignin was determined gravimetrically. A thermogravimetric (TG) analyzer (SDT 650) was used to measure thermostability in nitrogen oxides at a heating rate of 10 ℃ min^{-1}. Zeiss LSM 800 confocal laser scanning microscopy was used with an excitation laser at Ar 488/ over an emission range of 490–700 nm with a 20×EC Plan Neofluar objective (N.A. 0.5) and 40×EC Plan Neofluar objective (N.A. 1.3). Software v. 5.0 (Zeiss) was used to acquire multichannel fluorescence images of the materials.

2D Small- and Wide-angle X-ray scattering (SAXS and WAXS) characterization and data interpretation SAXS and WAXS experiments were performed using XEUSS 2.0 in-house SAXS/WAXS instrument (Xenocs SAS, Grenoble, France). The X-ray wavelength λ was 1.54 Å; and the sample-to-distance (SDD) was 586 and 132 mm for SAXS and WAXS, respectively. Miller indices of the reflections of possible cellulose polymorphs are given in Figure S6. The orientation of cellulose crystals was analyzed using the azimuthal scan of the scattered intensity in 2D WAXS patterns, as shown in Figure S7. Note that Figure S7 shows the WAXS pattern of natural bamboo, which is the same as shown in Figure S6A, but is annotated with the scheme of the azimuthal scan. ϕ denotes the azimuthal angle, ranging from $\phi = 0°$ to $\phi = 90°$ (fiber direction is aligned with the direction of $\phi = 90°$). The scattered intensities in the vicinity of the (200) reflection (within the circles of the dashed line) are averaged and plotted against ϕ. The intensity distribution is symmetric, so we used the mirror image of the data between $\phi = 0°$ and 90° to represent that between $\phi = -90°$ and 0°, hence showing the bell-shaped profile.

The degree of fibril crystal orientation can be quantified using Hermans's orientation factor, P_2, which is defined in Eq. Sp1. P_2 varies between 0 and 1, with 0 referring to a status of random orientation, and 1 to the condition of perfect fibril alignment.

$$P_2 = \frac{1}{2}\left(3\langle cos^2\phi\rangle - 1\right) \quad \text{(Eq. Sp. 1)}$$

2D HSQC NMR test characterization and calculation The 2D HSQC NMR experiments were performed on whole plant cell walls and enzyme lignin (EL) as previously described (Kim et al., 2008; Kim and Ralph, 2010; Kim et al., 2017). Each ball-milled whole cell wall (50 mg) was directly prepared in NMR tubes for gel-state NMR experiments using DMSO-d_6: pyridine-d_5 (4:1, v/v). Each EL (20 mg) was also prepared using the same solvent system. The central DMSO solvent peak (δC 39.5, δH 2.49 ppm) was used as the internal reference. The NMR data were

acquired on a Bruker Biospin (Billerica, MA) Avance NEO 700 MHz spectrometer equipped with a 5 mm QCI $^{1}H/^{31}P/^{13}C/^{15}N$ cryoprobe with inverse geometry.

All NMR experiments used Bruker's standard pulse programs, and an adiabatic $^{1}H–^{13}C$ 2D HSQC experiment (hsqcetgpsisp2.2) was conducted as described in previous publications (Kim and Ralph, 2010; Kim et al., 2017). F. For the EL samples, the HSQC experiments were acquired from 11.5 to −0.5 ppm (12 ppm spectral width) in F2 (^{1}H) with 3,366 data points (acquisition time, 200 ms) and 215 to −5 ppm (220 ppm spectral width) in F1 (^{13}C) with 618 increments (F1 acquisition time, 8.0 ms) of 24 scans with a 1 s interscan delay (D1); the d24 delay was 0.89 ms (1/8J, J = 145 Hz). The total acquisition time for a sample was 5 h. The same experimental ranges were acquired for the whole-cell-wall samples but acquired with 1,724 data points (acquisition time of 100 ms) in F2 and 618 increments (acquisition time of 8 ms) in F1. The number of scans (NS) was 56 with a 500 ms interscan delay (D1). The total acquisition time for each was 6 h.

The data were analyzed based on the previous reports (Kim and Ralph, 2010; Kim et al., 2017). The volume integration of contours in HSQC plots was performed using TopSpin 4.1.4 software (Mac version) from Bruker, and no correction factors were used. For quantification of aromatic H/G/S signals, the $H_{2/6}$ and $S_{2/6}$ correlations were used, and the G_2 integrals were doubled to be on the same atom basis ($S_{2/6} + S'_{2/6} + H_{2/6} + 2G_2 = 100\%$). For the estimation of the various aliphatic interunit linkage types, the well-resolved α-C/H peaks were measured, and the relative percentages are reported. As such, the data is presented on a $2A_\alpha + 2B_\alpha + C_\alpha = 100\%$ basis (A = β-ether, B = phenylcoumaran, and C = resinol).

Mechanical tests A Tinius Olsen H5KT tester was used to measure the shear and tensile characteristics of the bamboo samples. For the measurement, the joint strength as a force per unit

area is measured in MPa (or N/mm^2) under a shear load (lap shear strength). The shear strength was calculated using the following equation:

$$Bonding\ strength\ (MPa) = \frac{tension\ force(N)}{gluing\ area(m^2)} \quad \text{(Eq. Sp. 2)}$$

Shear samples were approximately 60 mm by 10 mm in size. At room temperature, a sample was clamped at both ends and stretched along the sample length direction until the two pieces separated at a constant test speed of 5 mm min^{-1}. The maximum shear force acting parallel to the direction of bamboo fiber is defined as shear stress. Tensile samples were approximately 90 mm by 10 mm in size. A sample was clamped at both ends and stretched along the sample length direction until it fractured at a constant test speed of 5 mm min^{-1}.

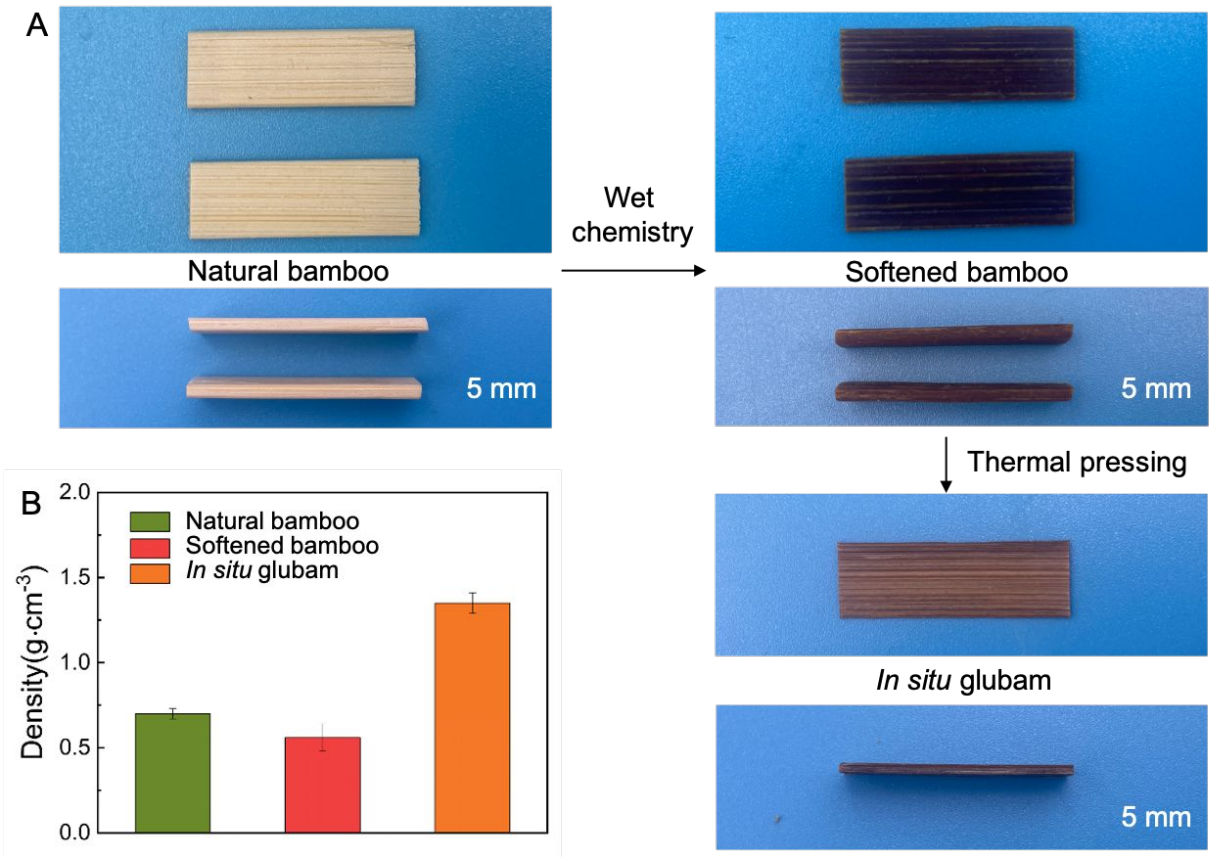

Figure S1. A) The fabrication process of the *in situ* glubam. Two natural bamboo strips with dimensions of approximately 30.0 mm by 10.0 mm by 2.0 mm were cut parallel to the bamboo growth direction. After wet chemistry treatment, the softened bamboo strips were washed with water to completely remove chemical waste until the pH = 7. We then hot-pressed the softened bamboo strips together into one piece of *in situ* glubam. B) Density of the natural bamboo, softened bamboo, and *in situ* glubam.

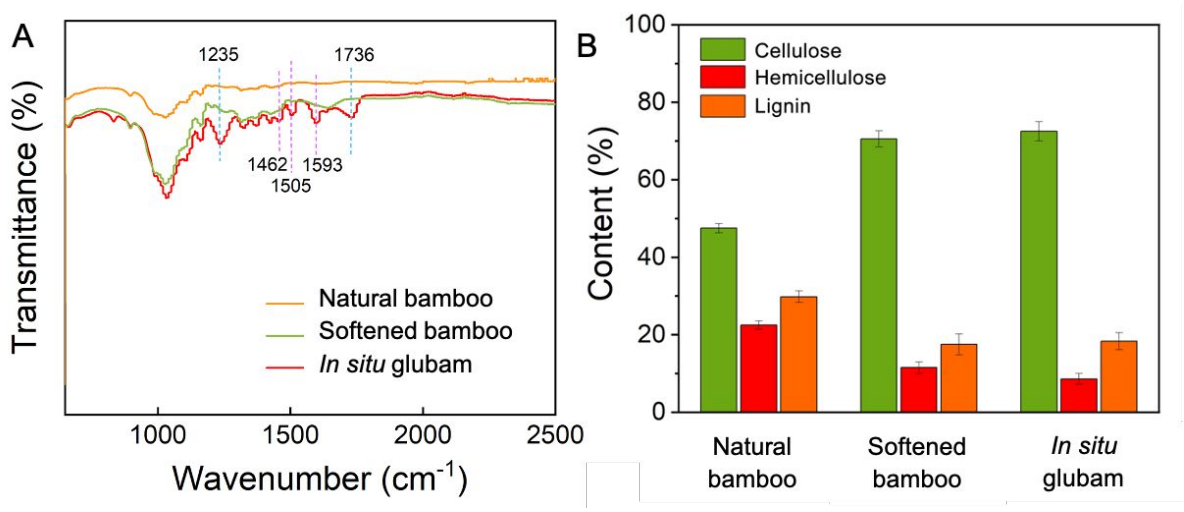

Figure S2. A) FTIR spectra and B) the corresponding composition of the natural bamboo, softened bamboo, and *in situ* glubam.

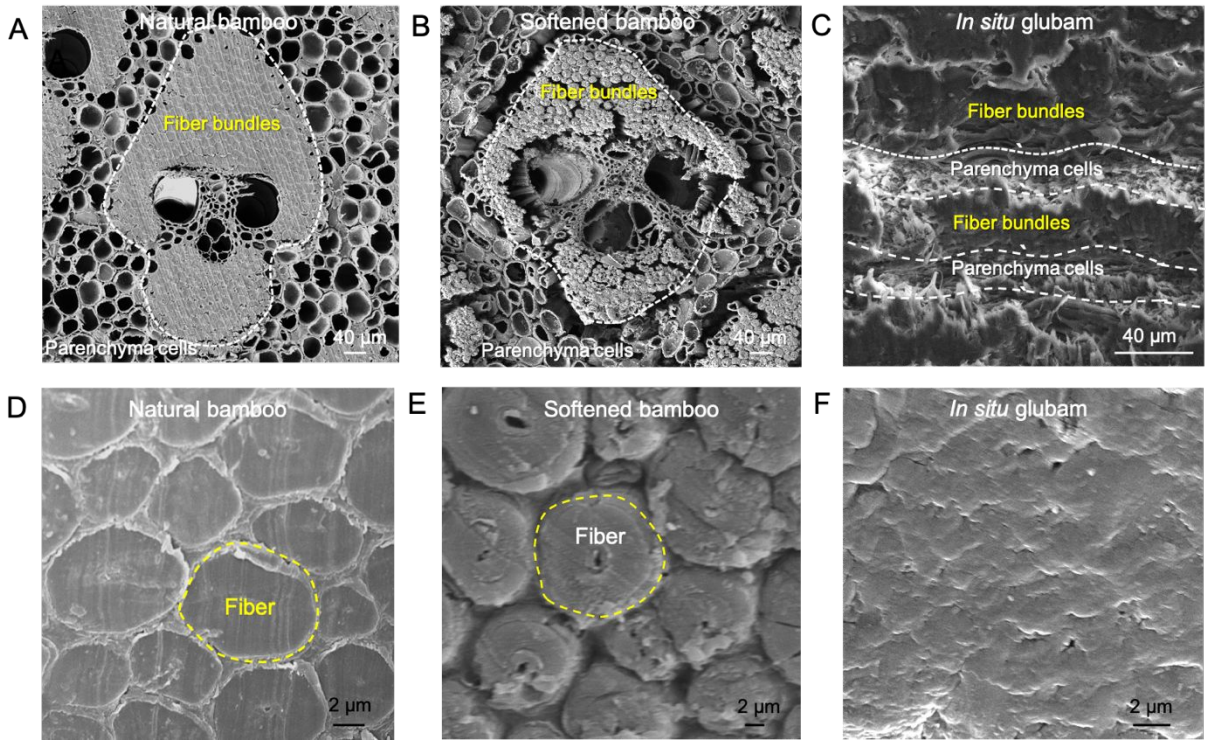

Figure S3. Cross-sectional SEM images of the A) natural bamboo, B) softened bamboo and C); *in situ* glubam. Magnified cross-sectional SEM images of D) natural bamboo fibers, E) softened bamboo fibers, and F) *in situ* glubam fibers.

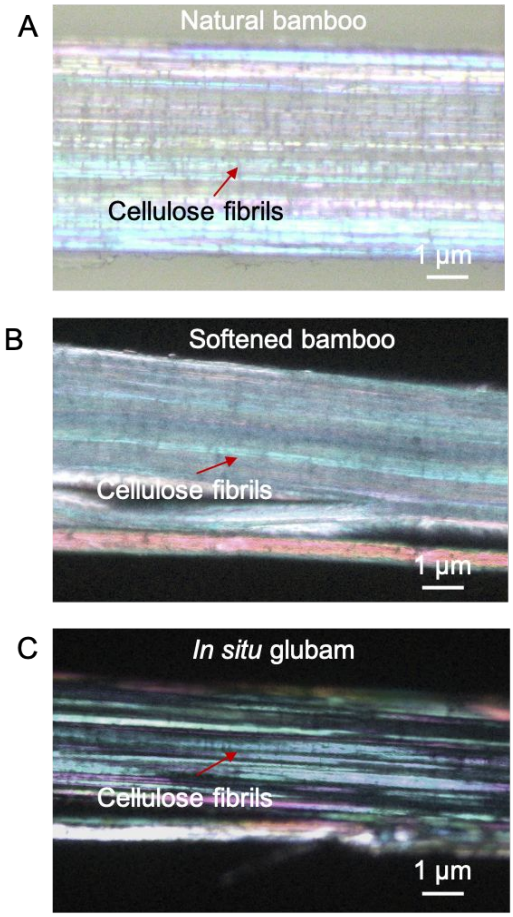

Figure S4. Polarized light microscopy images of the fibers of A) the natural bamboo, B) softened bamboo, and C) *in situ* glubam. The bright birefringence is reflected by the cellulose nanofibrils under polarized light.

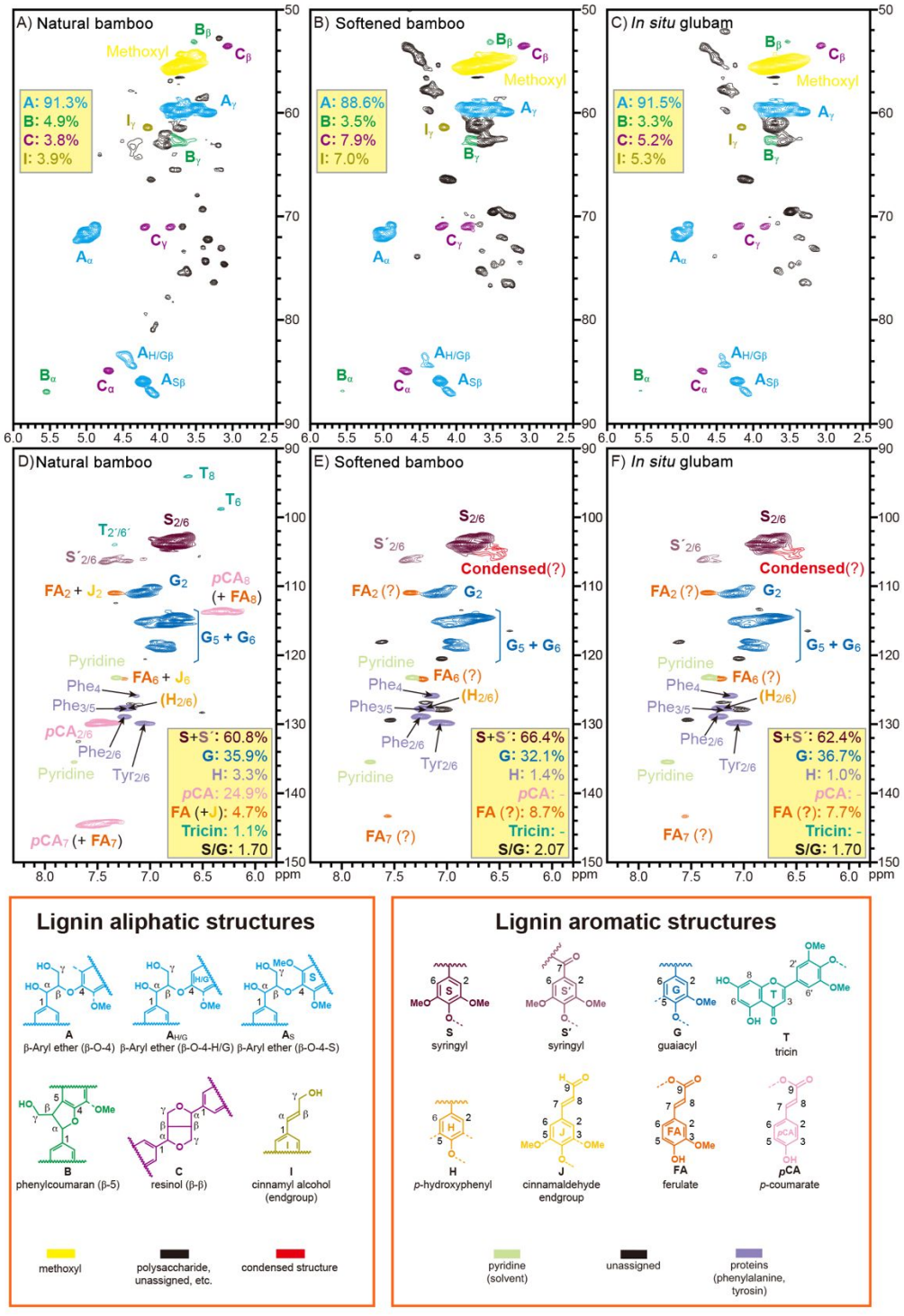

Figure S5. 2D HSQC NMR spectra of lignin aliphatic regions (δC/δH 50–90/2.4–6.0) of A) natural bamboo, B) softened bamboo, and C) *in situ* glubam. 2D HSQC NMR spectra of lignin aromatic regions (δC/δH 90–150/5.8–8.3) of D) natural bamboo, E) softened bamboo, and F) *in situ* glubam.

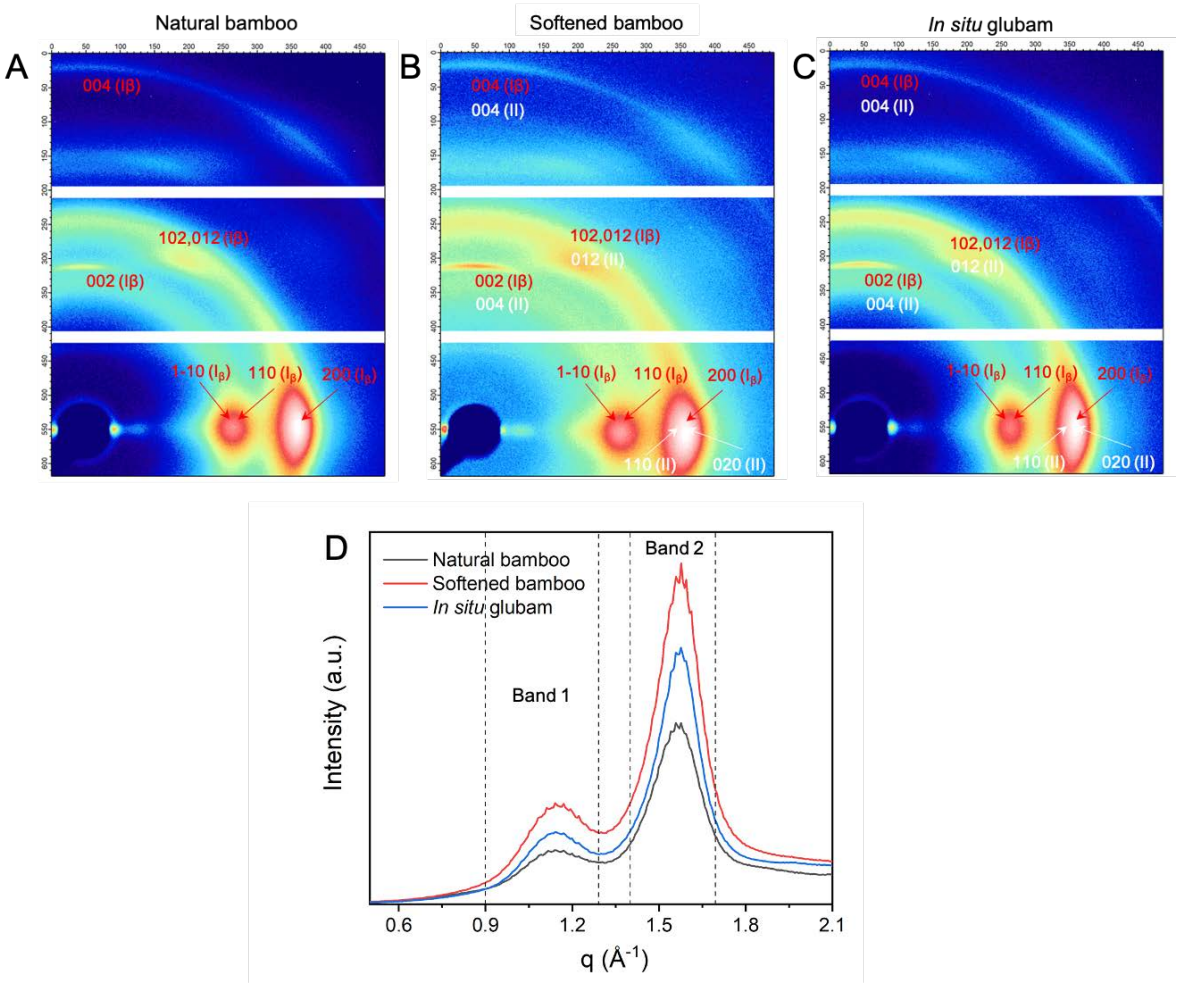

Figure S6. The 2D-WAXS patterns of the A) natural bamboo B) softened bamboo and C) *in situ* glubam. D) One-dimensional scattering profiles of natural bamboo, softened bamboo, and *in situ* glubam. The profiles are reduced from a wedge in the equator direction of the 2D WAXS patterns, representing contributions from (hk0) reflective planes. Diffraction peaks are grouped into two bands, denoted as band 1 and band 2, Diffraction peaks are grouped into two bands, denoted as band 1 (0.9 ~1.3 $Å^{-1}$) and band 2 (1.4 ~1.7 $Å^{-1}$).

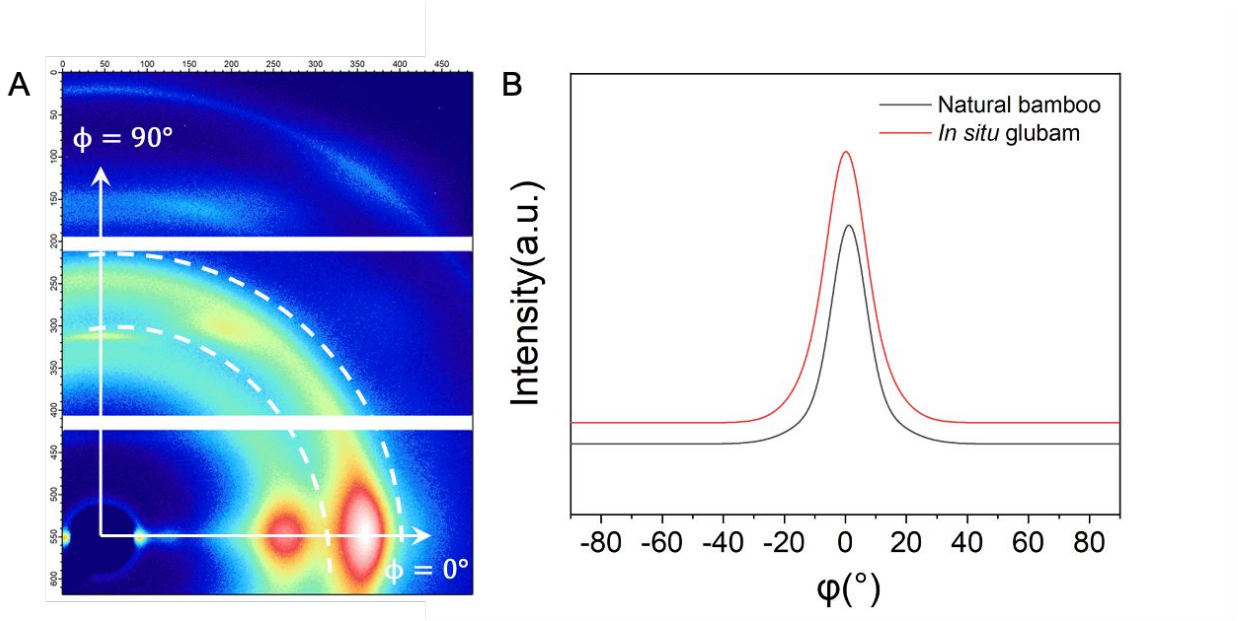

Figure S7. 2D-WAXS pattern of the natural bamboo annotated to show the scheme of the azimuthal angle scan for crystal orientation analysis A) Reference azimuthal angles at ϕ = 0° and 90° are indicated. Scattered intensity banked between the dashed line (including the (200) reflection as shown in Figure S6) is averaged and plotted against the ϕ (B). The breadth of the scattered intensity distribution in B) is an indicator of fibril crystal orientation degree, quantified using Hermans's orientation function (see the text for details).

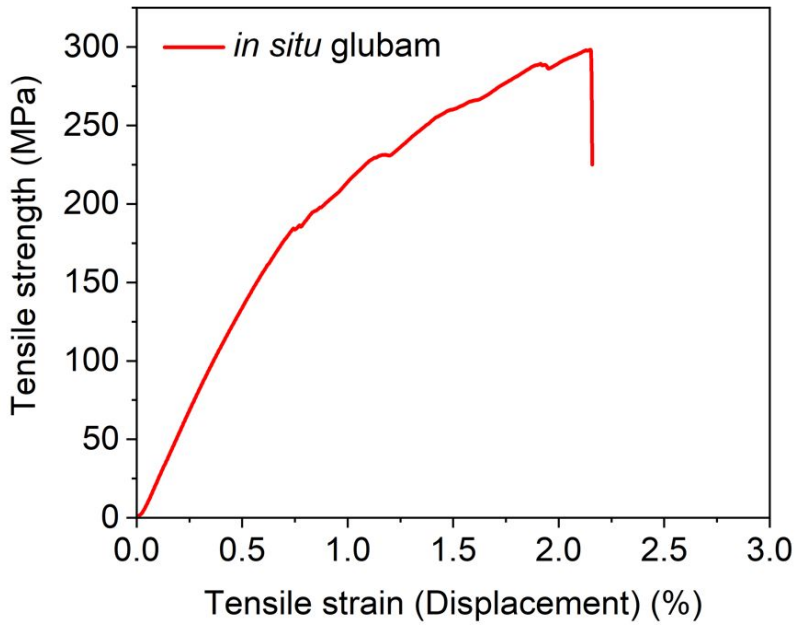

Figure S8. Tensile strength−strain curves of i*n situ* glubam.

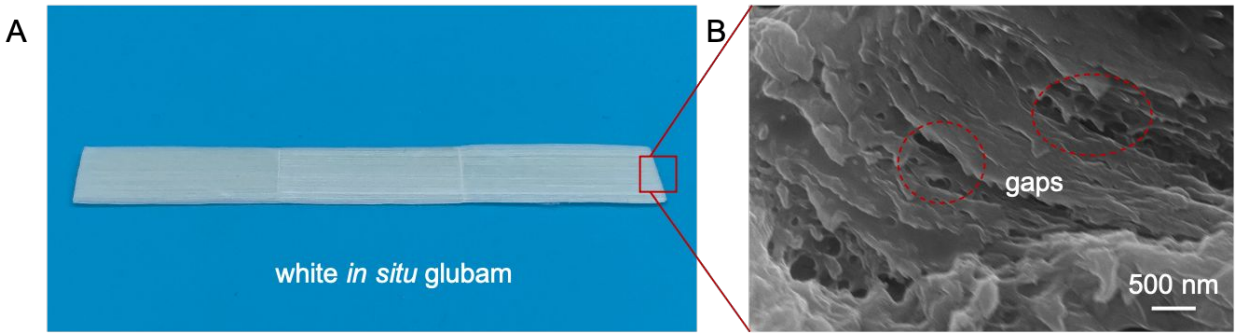

Figure S9. A) Optical and B) SEM images of 0%-lignin *in situ* glubam, showing many gaps between the cellulose fibers owing to the absence of lignin as a binding agent.

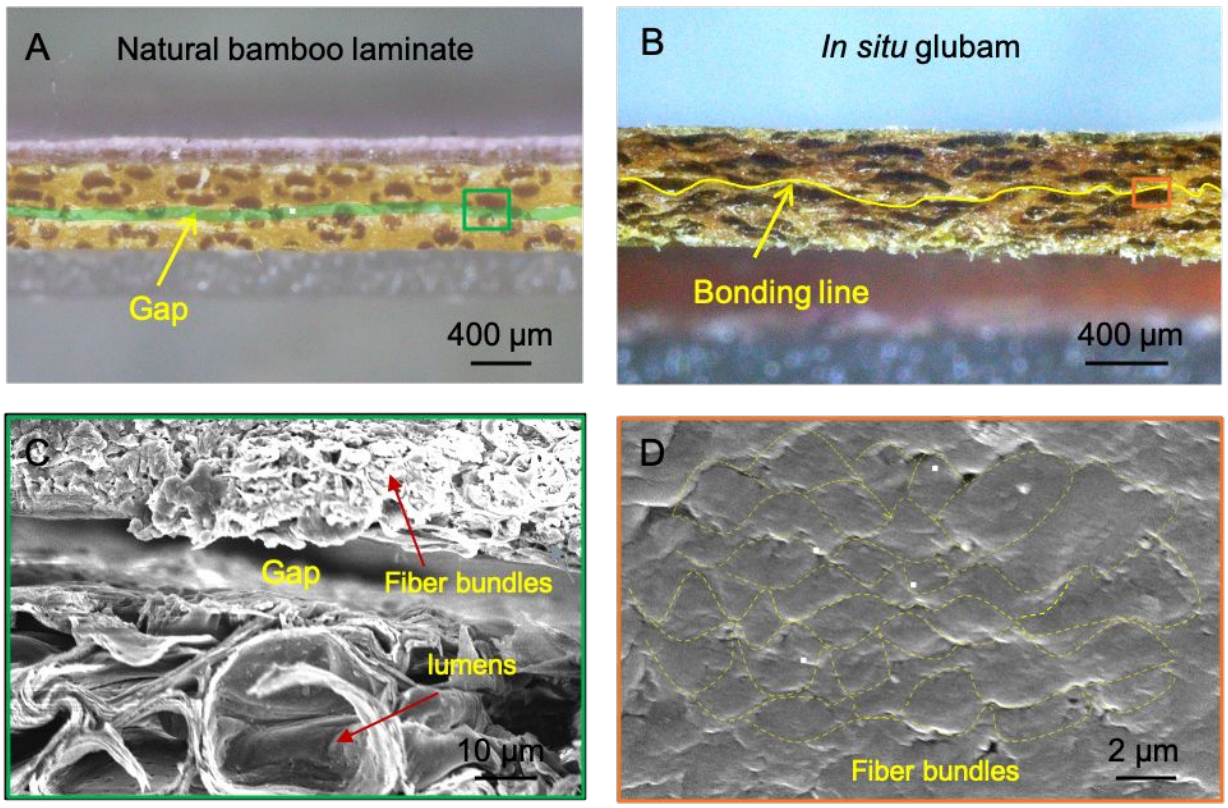

Figure S10. Cross-sectional images of the A) natural bamboo laminate and B) *in situ* glubam. Cross-sectional magnified SEM images of the C) natural bamboo laminate, which show gaps remaining in the partially collapsed lumens and fiber bundles, while D) the *in situ* glubam features totally collapsed fiber bundles.

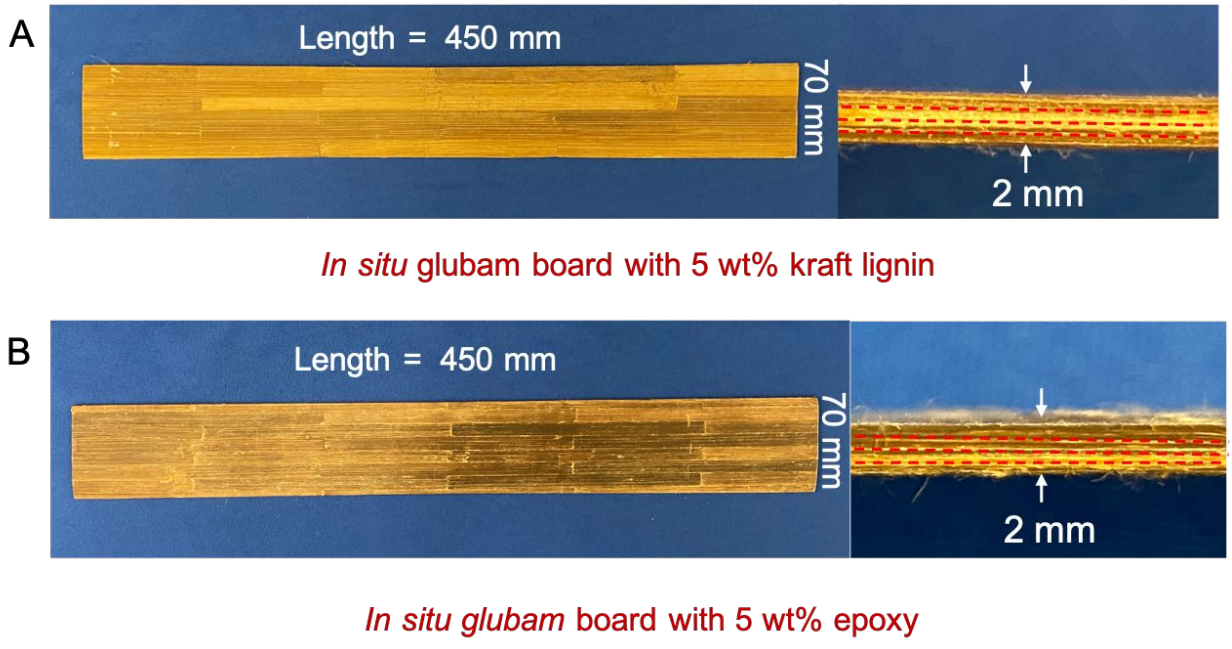

Figure S11. *In situ* glubam board enhanced by adding A) kraft lignin and B) epoxy, separately.

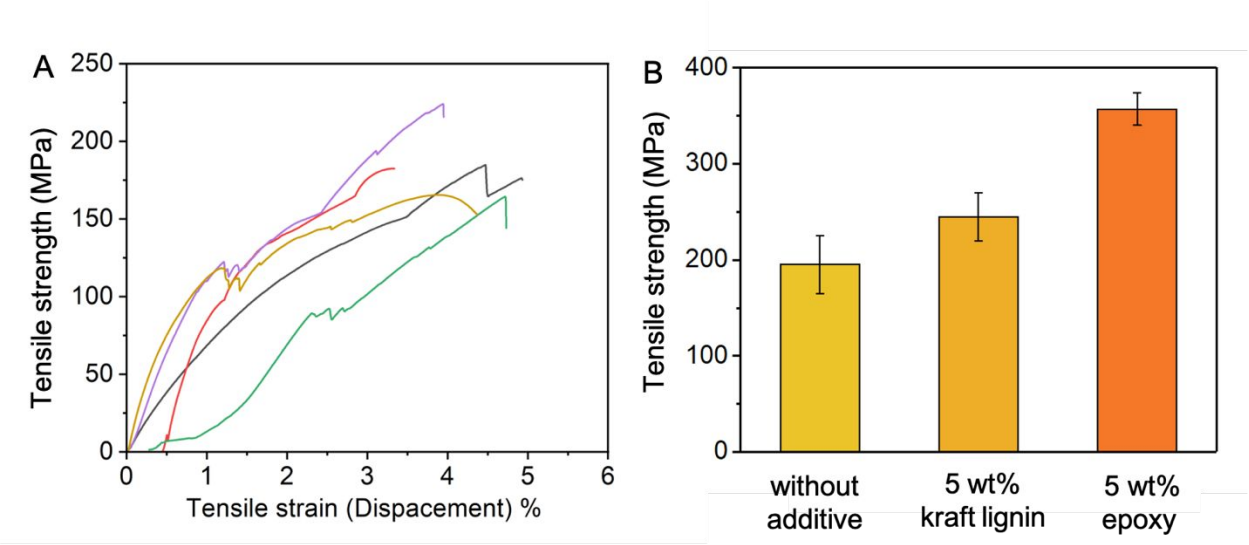

Figure S12. A) Stress-strain curves of randomly selected small samples containing nodes from a large *in situ* glubam board, which feature a similar tensile strength of ~195 ± 30 MPa. B) The tensile strength of the *in situ* glubam board without additive, adding 5 wt% kraft lignin and 5 wt% epoxy, separately.